Image Acquisition and Reconstruction

11.6.2018

Jarmo Teuho, PhD

(Medical Physics and Engineering)

Specialist Researcher

Turku PET Centre

University of Turku and Turku University Hospital

Turku, Finland

jarmo.teuho@tyks.fi

Learning objectives

After the the lecture the student should know the basic concepts of

- **Data acquisition: line-of-response, coincidence detection, 2D and 3D, non-tof vs tof differences**
- **Data representation: list-mode data, sinograms, michelogram**
- **Reconstruction workflow: from raw data to images, data corrections, practical example**
- **Analytical and iterative reconstruction algorithms: FBP, MLEM, OSEM**

Definitions

- LOR = Line of response connecting two detectors
- TOF = Time of flight
- List-mode data, sinogram, michelogram = PET raw data used for data representation and reconstruction
- FBP = Filtered BackProjection, analytical reconstruction algorithm
- MLEM = Maximum Likelihood Expectation Maximum, iterative reconstruction algorithm
- OSEM = Ordered Subset Expectation Maximum, iterative reconstruction algorithm, a derivate of MLEM

Further information

Contact people at Turku PET Centre

- **PhD Jarmo Teuho (jarmo.teuho@tyks.fi)**
- **Professor Mika Teräs (mika.teras@tyks.fi)**

STIR/SIRF

- http://stir.sourceforge.net/
- https://www.ccppetmr.ac.uk/node/1

NiftyRec

- http://niftyrec.scienceontheweb.net/wordpress/

ASIM/SIMSET

- http://depts.washington.edu/simset/html/user_guide/user_guide_index.html
- https://depts.washington.edu/asimuw/

GATE/GEANT

- http://www.opengatecollaboration.org/

Homepage of J.Fessler:

- https://web.eecs.umich.edu/~fessler/

Handbook of Nuclear Medicine Imaging:

- https://www-pub.iaea.org/MTCD/Publications/PDF/Pub1617web-1294055.pdf

PET Data Acquisition

- Line-of-response
- Coincidence detection
- 2D vs 3D acquisition
- Non-TOF system vs TOF system

Line of Response

- A straight line which connects the centers of two detectors X and Y is called a line of response (**LOR**).
- The two 511 keV photons are detected in coincidence across a LOR, in the absence of an absorptive collimator.
- This technique is called **electronic collimation.**
- All coincident events recorded are collectively called as prompt events, containing:
  - True events
  - Random events
  - Scattered
  - Multicoincidence
  - Motivation for data corrections

Coincidence Detection

- Creation of two electronic pulses (at detectors X and Y) at the same time ("in coincidence") signifies a point of annihilation *somewhere* in the LOR connecting the associated detectors X and Y.
- During the scan, coincidence counts are recorded for each LOR and stored in a raw data format (list-mode or sinogram).
- The number of coincidence counts obtained on a particular LOR indicates amount of radioactivity ("counts") present along that line during the scan.
- A parallel set of LORs through the imaged object f(x,y) can be collected as a set of projections $p(s,\phi)$ of the radioactivity distribution. The collection of all these projections is called a sinogram.

From Coincidence to Raw Data

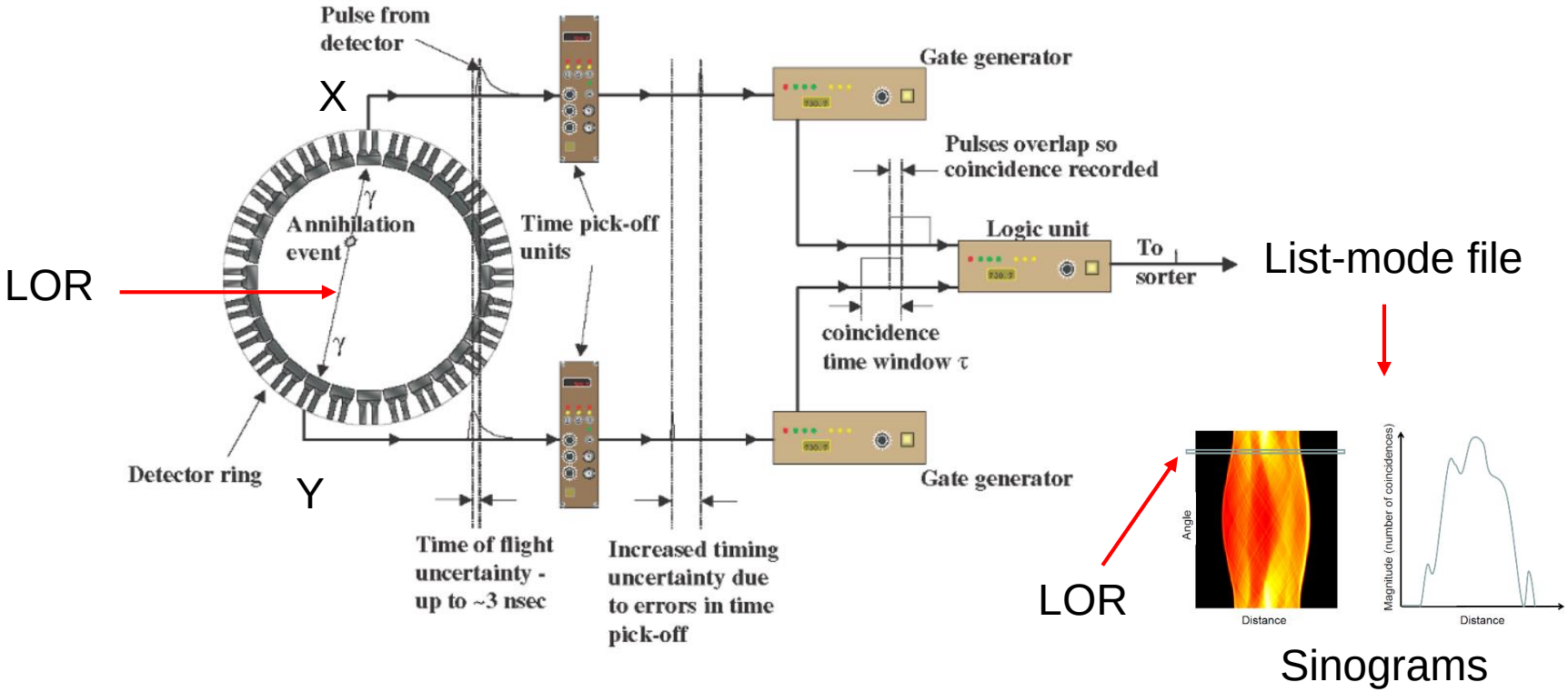

Figure 5.2. Figure 5.2 Example coincidence circuitry. Each detector generates a pulse when a photon deposits energy in it; this pulse passes to a time pick-off unit. Timing signals from the pick-off unit are passed to a gate generator which generates a gate of width τ. The logic unit generates a signal if there is a voltage on both inputs simultaneously. This signal then passes to the sorting circuitry.

Modified from : Quantitative Techniques in PET
Steven R Meikle and Ramsey D Badawi

2D Data vs 3D Data Collection

$$p(x_r, \varphi) = \int_{-\infty}^{\infty} f(x, y)\, dy_r$$

2D

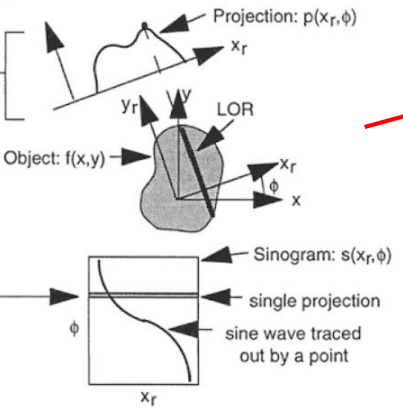

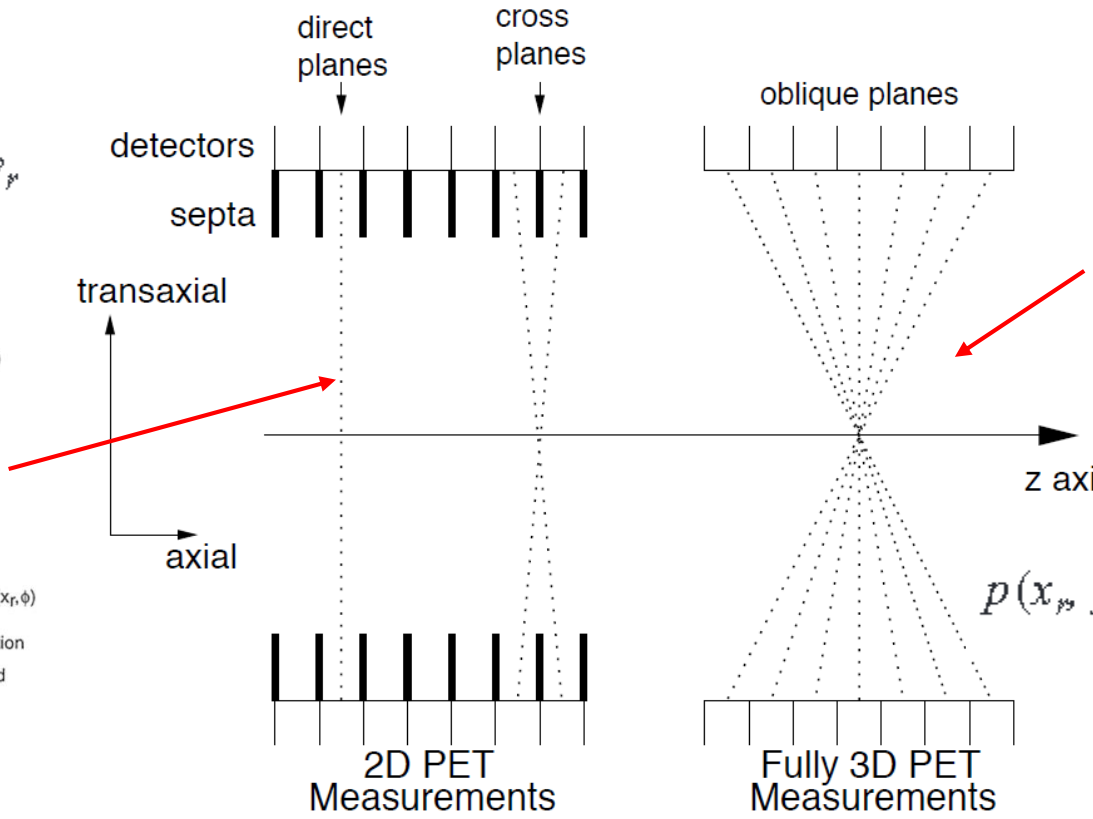

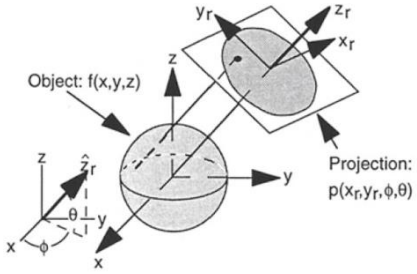

3D

$$p(x_r, y, \varphi, \vartheta) = \int_{-\infty}^{\infty} f(x, y, z)\, dz_r$$

Figure 4. Comparison of fully 3-D and 2-D PET measurements. In 2-D mode, scanner only collects direct and cross planes (organized into direct planes). In fully 3-D mode, scanner collects all, or most, oblique planes.

PET Image Reconstruction
Adam Alessio and Paul Kinahan

The Theory and Practice of 3D PET
Bendriem, B., Townsend, D.W.

Line-of-Response in TOF and non-TOF

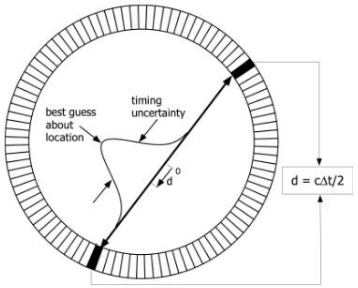

Fig. 4b. Coincidence processing in time-of-flight (TOF) PET data acquisition.

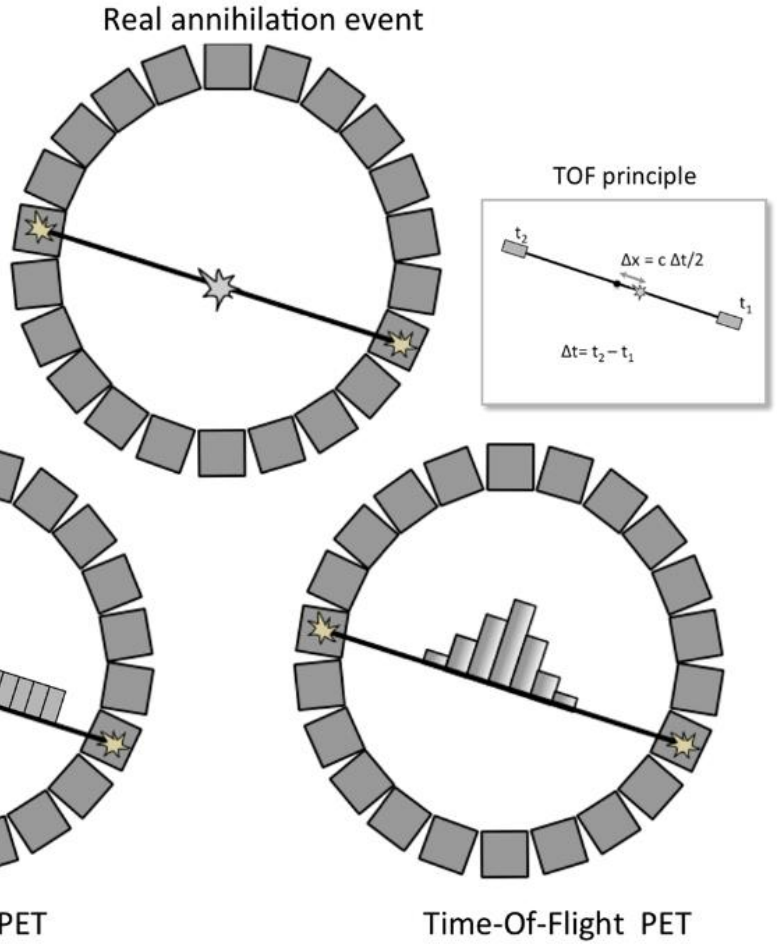

Non-TOF PET, the probability of detection is assumed uniform across the LOR

In TOF PET the arrival-time difference of the two detected photons is measured.

Time difference is used to determine the most likely location (d) of the annihilation event.

Data Representation

- List-mode data
- Sinogram
- Michelogram

List-mode data

- In list-mode acquisition, digitized X- and Y- signals are coded with "time marks" as they are received in sequence.
- Signals are stored as individual events as they occur.
- After the acquisition is completed, data can be histogrammed to individual sinograms.
  - Other terms: data sorting, unlisting, sometimes re-binning
- This way of storing the data allows flexibility, since the data can be sorted to sinograms as:
  - Static (whole scan time e.g. 15 minutes)
  - Dynamic (by time to shorter frames e.g. 3x180 s, 5x300 s, etc.)
  - Gated (respiratory or cardiac time marks e.g. by respiratory or cardiac phase)
- Practical hurdles:
  - Size and storage requirements (1,5 GB for non-TOF and 4 GB+ for TOF)
  - Increased activity / sensitivity => disk writing speed + memory/storage requirements

Visual Representation of List-mode data

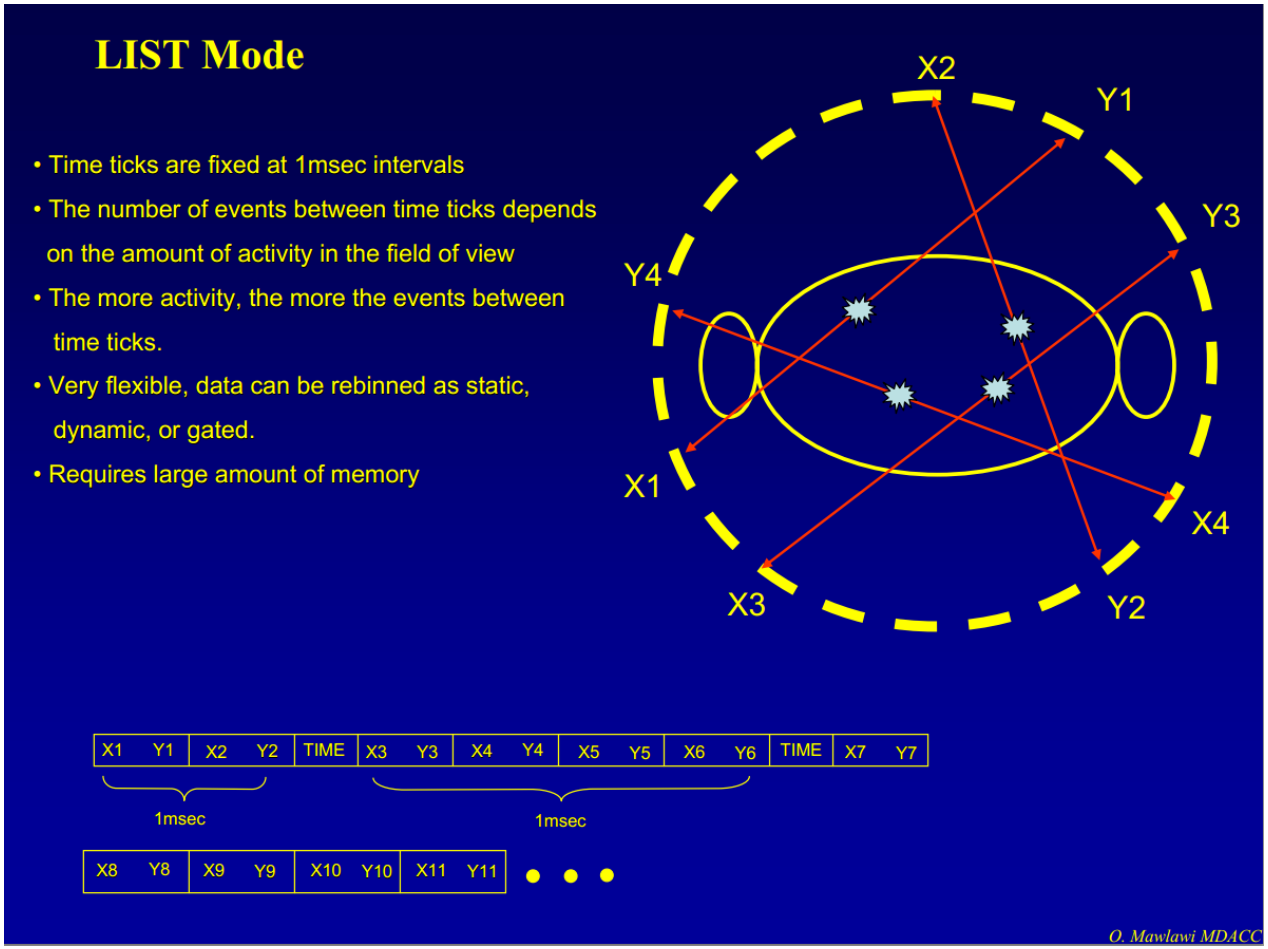

https://www.aapm.org/meetings/amos2/pdf/42-11881-66890-783.pdf

Sinogram

- It is typical to store and display the raw data in a sinogram.
- The imaged object f(x,y) is now collected as a set of projections p(s,ϕ) of the radioactivity distribution.
- In essence, by performing image reconstruction we want to recover the original imaged object f(x,y) from this set of projections p(s,ϕ).
- The line-integral transform of f(x,y) to p(s,ϕ) is called the X-ray transform, or the **Radon transform** in 2D. During image reconstruction process, this is usually referred as *forward projection* operation while *backprojection* is the adjoint operation of forward projection (**inverse Radon transform**).

Sinogram Formation, Forward Projection

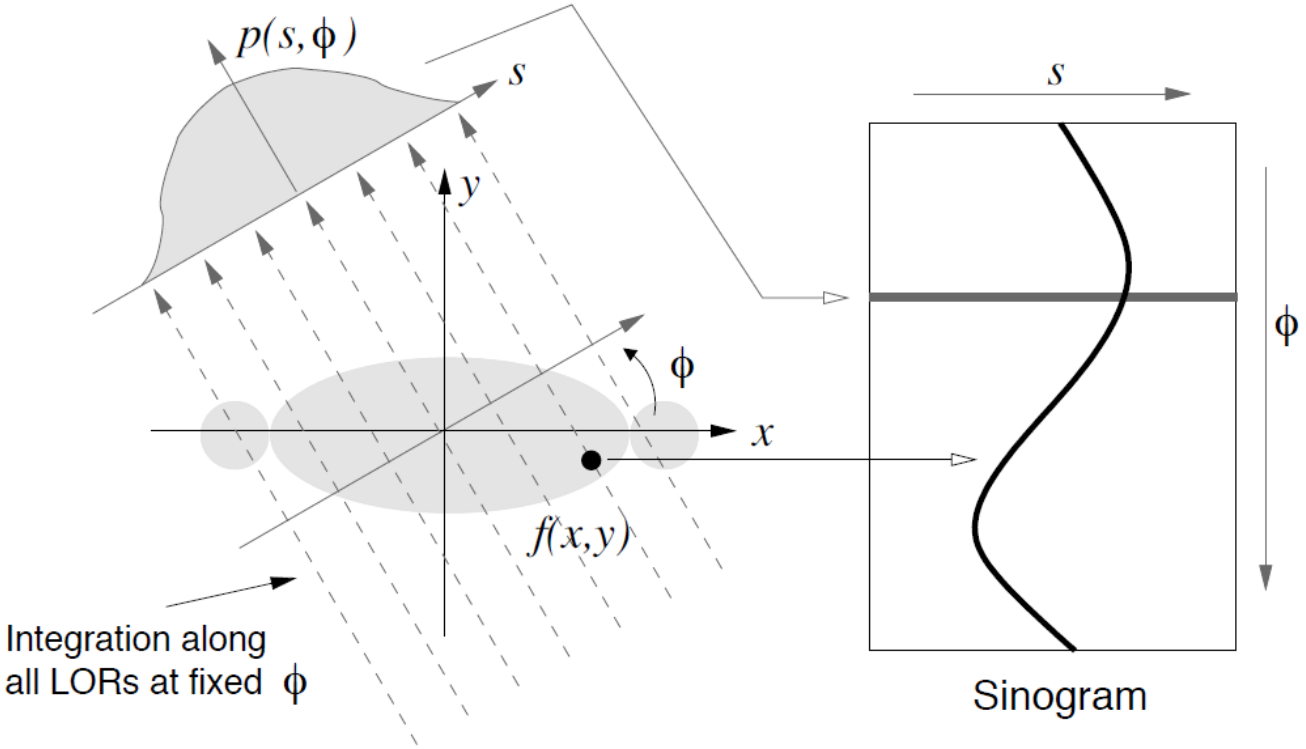

Figure 2. A projection, $p(s,\phi)$, is formed from integration along all parallel LORs at an angle ϕ. The projections are organized into a sinogram such that each complete projection fills a single row of ϕ in the sinogram. In this format, a single point in $f(x,y)$ traces a sinusoid in the sinogram.

PET Image Reconstruction
Adam Alessio and Paul Kinahan

Backprojection

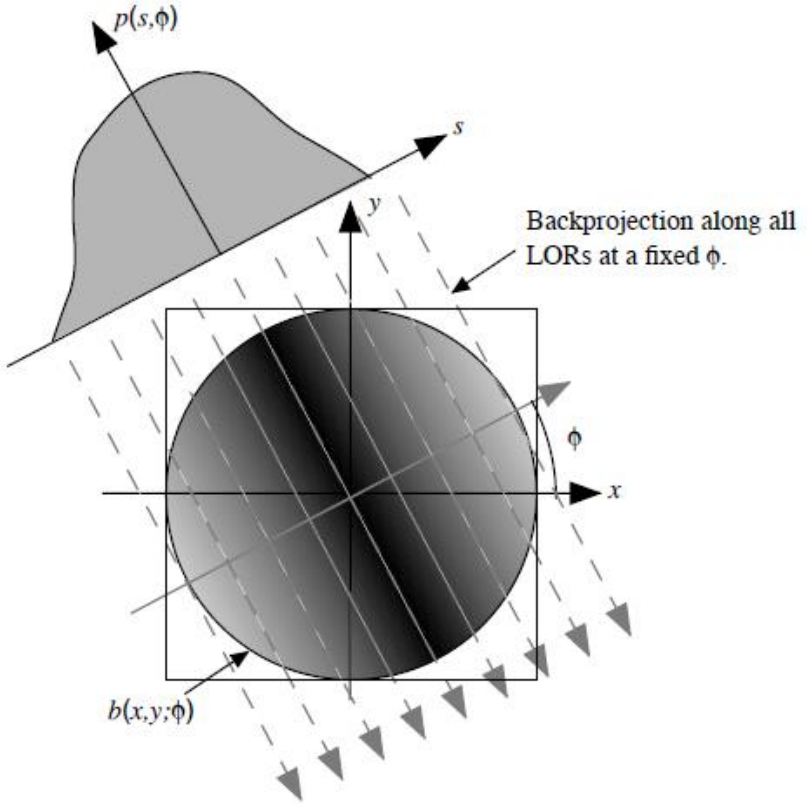

Figure 6. Backprojection, $b(x,y;\phi)$, into an image reconstruction array of all values of $p(s,\phi)$ for a fixed value of ϕ.

PET Image Reconstruction
Adam Alessio and Paul Kinahan

Sinogram in 2D Acquisition and Reconstruction

- In projection space, the imaging volume is described as $p(s,\phi,z,\theta)$
- In the 2D case all data are sampled (or assumed to be sampled) with polar angle $\theta = 0°$, where projections $p(s,\phi,z)$ are formed only for a single transverse slice at a time of the volumetric object $f(x,y,z)$.
- The volumetric object $f(x,y,z)$ is recovered by reconstruction of each 2D sinogram $p(s,\phi,z)$ corresponding to an individual slice z, leading to an 3D image. Stack of sinograms => individual slices => imaged 3D object.
- The image reconstruction process starts with collected & uncorrected raw data (typically sinograms), performs essential data corrections and tries to recover the cross-sectional images that represent radioactivity distribution inside the imaged object.

Practical Example
One 2D Sinogram

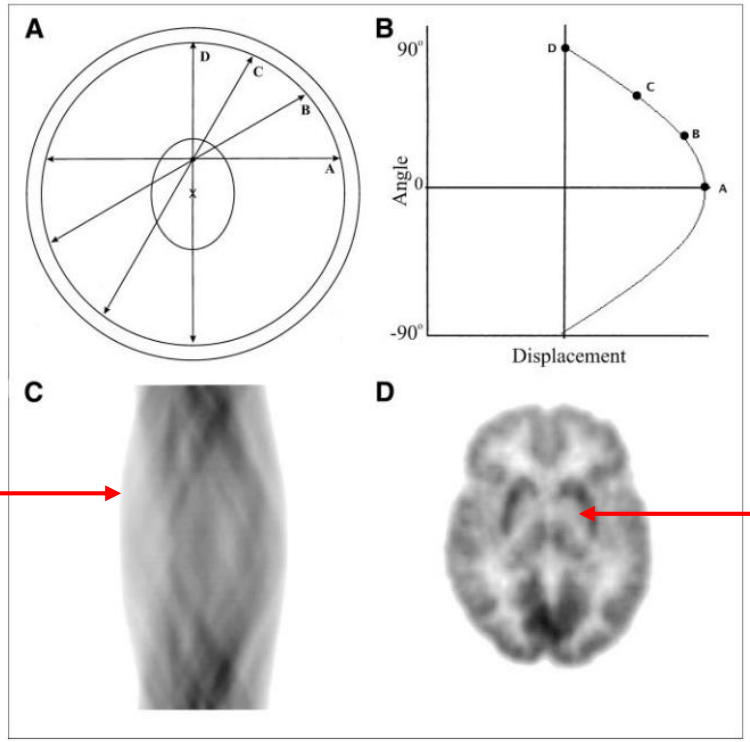

The sinogram is a two-dimensional histogram of the LORs in distance and angle coordinates

Each sinogram represents the data acquired for a slice across all angles

After data corrections and image reconstruction, the image is a pixel-by-pixel representation of the radiotracer concentration at scan time.

FIGURE 1. Sinogram formation. Coincidence events in PET scanner are categorized by plotting each LOR as function of its angular orientation versus its displacement from center of gantry. (A) Center of gantry is noted by cross (X), and locus of interest (e.g., tumor) is noted by ellipse. Four LORs passing through locus of interest are labeled A, B, C, and D. (B) These 4 LORs are plotted on this sinogram where angular orientation is on *y*-axis and displacement from center of gantry is on *x*-axis. If all possible LORs that pass through this point are plotted, it maps out half of sine wave turned on its side as shown here. (C) Sinograms of more complicated objects, such as sinogram of brain scan shown, are composed of many overlapping sine waves. (D) Reconstructed brain image corresponding to sinogram in (C) is shown.

Data Acquisition in PET Imaging, Frederic H. Fahey

Sinogram in 3D Acquisition and Reconstruction

- In the 3D case, the sinograms $p(s,\phi,z,\theta)$ are extended to measuring projections at polar angles $\theta > 0°$ (oblique or tilt angles).

- In 3D data, the acquired LORs are represented in terms of four parameters, s, ϕ, θ and z, which denote:
  - the radial distance s
  - rotation angle ϕ
  - oblique or tilting angle θ
  - shift in the axial direction z

- A 2D reconstruction algorithm can also be applied to 3D data by rebinning the data to individual 2D sinograms:
  - Single-slice rebinning (SSRB), fourier rebinning (FORE, e.g. FORE-FBP, FORE-OSEM)

- Naturally, a fully 3D reconstruction algorithm can be applied (iterative or analytical). There are specific considerations when using analytical algorithms for 3D data, as some of the projections are truncated.
  - The interested reader is referred to e.g.: Image Reconstruction Algorithms in PET, Michel Defrise, Paul E Kinahan and Christian J Michel

Michelogram

- A graphical representation was introduced by the Belgian scientist Christian Michel to illustrate the plane definitions used in a large multi-ring PET system - known as "**Michelogram**" representations.
- A michelogram illustrates how different planes can be combined to optimize storage space and data-handling requirements.
- In 3D-PET sinograms from direct and crossing planes can be merged to additionally reduce the data volume, effectively resulting in an axial compression (span). Axial and angular compression is performed by the scanner hardware during the data acquisition process.
- The interested reader is referred to:
  - Image Reconstruction Algorithms in PET, Michel Defrise, Paul E Kinahan and Christian J Michel
  - Data Acquisition in PET Imaging, Frederic H. Fahey
  - Data Acquisition and Performance Characterization in PET, Dale L Bailey

Michelogram Example 2D PET, span 7

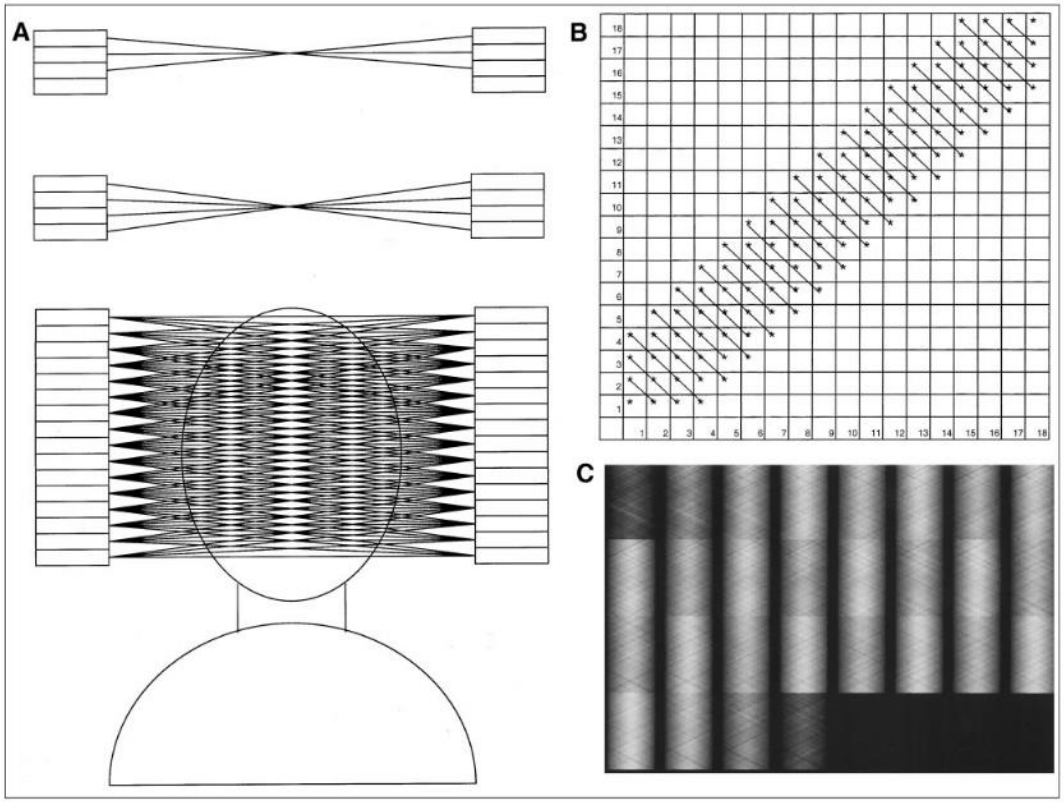

FIGURE 7. 2D PET with span of 7. (A) Top of figure shows configuration for odd-numbered slices. Not only is direct LOR used but also 2 cross LORs on either side of it. For example, Ring 2 in coincidence with Ring 2, Ring 3 with Ring 1 and Ring 1 with Ring 3. For even-numbered slices, 2 sets of cross LORs are used (e.g., Ring 2 to Ring 3, Ring 3 to Ring 2, as well as Ring 1 to Ring 4, and Ring 4 to Ring 1). Since odd-numbered planes contain 3 LORs and even ones contain 4, this is referred to as span of 7. (B) Michelogram for 16-ring scanner using span of 7. (C) Set of sinograms corresponding to Michelogram in (B) that have not been corrected for detector sensitivity or plane

Data Acquisition in PET Imaging, Frederic H. Fahey

Michelogram Example, 2D and 3D PET

2D

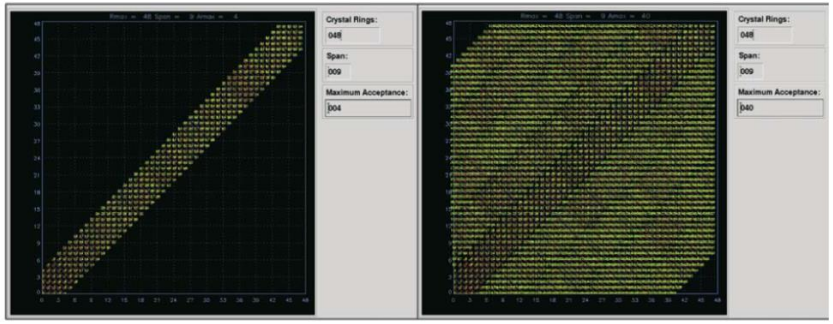

3D

Figure 3.8. Michelograms representing the plane combinations for a 48-ring scanner are shown for the 2D case (left) and the 3D case (right). The x and y axes represent ring numbers on opposing sides of the scanner. Each point on the graph defines a unique plane of response (e.g., all lines-of-response in ring 1 in combination with ring 2).The diagonal lines joining individual dots indicate that the planes of response are combined (added together) thus losing information about each individual point's polar acquisition angle. This form of combination of data from different planes represents a "lossy" compression scheme.

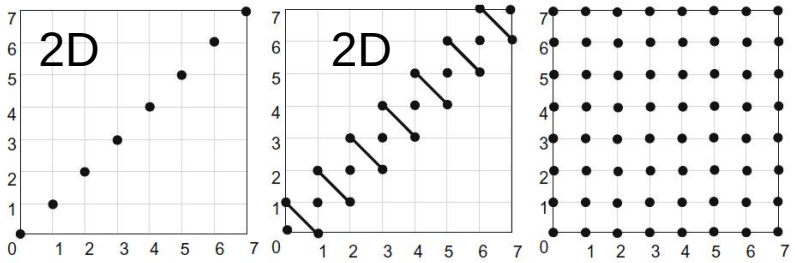

3D

Figure 3.7. The graphical Michelogam is shown for three different acquisition modes on a simple eight-ring tomograph. Each point in the graph represents a plane of response defined between two sets of opposed detectors (a sinogram). In the graph on the left (a simple 2D acquisition with no "inter-planes"), the first plane defined is ring 0 in coincidence with the opposing detectors in the same ring, 0; ring 1 in coincidence with ring 1; etc, for all rings, resulting in a total of eight sinograms. In the middle graph, the same planes are acquired with the addition of a set of "inter-planes" formed between the rings with a ring difference of ±1 ring (ring 0 with ring 1, ring 1 with ring 0, etc). These planes are added together to form a single plane, indicated by the line joining them. This would lead to approximately twice the count rate in this plane compared with the adjacent plane which contains data from one ring only. Physically, this plane is positioned half way between detector rings 0 and 1. While the data come from adjacent rings they are assumed to be acquired with a polar angle of 0° for the purposes of reconstruction. This pattern is repeated for the rest of the rings. This results in 15 (i.e., 2N − 1) sinograms. This is a conventional 2D acquisition mode, resulting in almost twice the number of planes as the previous mode, improving axial sampling, and contributing over 2.5 times as many acquired events. In the graph on the right, a fully 3D acquisition is shown with each plane of data being stored separately (64 in total). The 3D mode would require a fully 3D reconstruction or some treatment of the data, such as a rebinning algorithm, to form 2D projections prior to reconstruction (see Ch. 4).

Data Acquisition and Performance Characterization in PET, Dale L Bailey

Reconstruction Workflow

- From raw data to PET images
- Data corrections
- Practical example with LM-OSEM

Uncorrected vs Corrected Sinogram

- In the process of image reconstruction we want to recover the original imaged object f(x,y) from a measured sinogram p(s,ϕ).
- However, to recover the original radioactivity distribution from the object, a set of **data corrections** need to be performed to the measured projection data
- In essence, the data corrections are implemented to account for physical effects and effects which occur due to detector geometry or sensitivity non-uniformity:
  - Attenuation and scatter correction
  - Detector geometry correction
  - Can also include effects such as resolution recovery (PSF modelling)
- It is essential that both the image acquisition process and data corrections are performed as accurately as possible, since all errors in the data acquisition process and correction process will propagate to the reconstructed PET images

From Raw Data to PET Images

Sort to sinograms

Data corrections

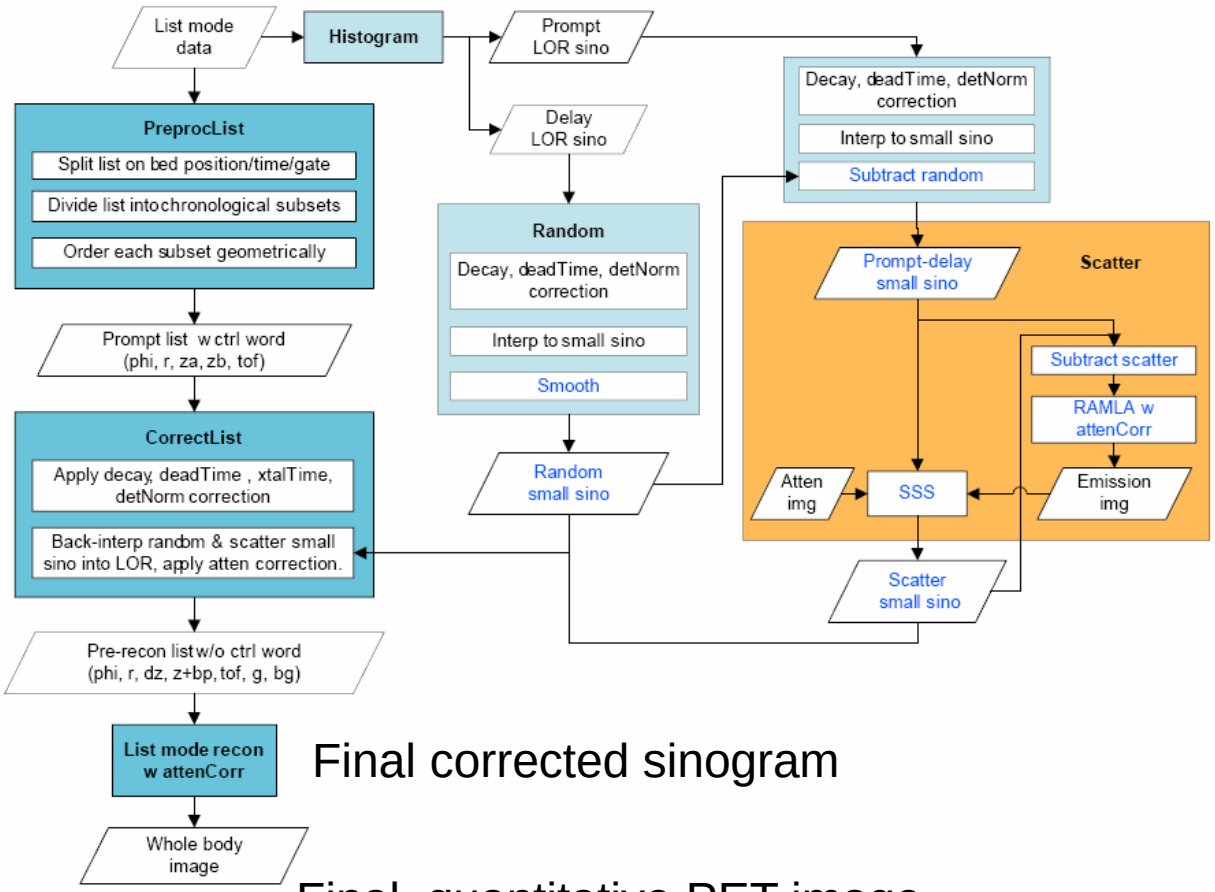

Final corrected sinogram

Final, quantitative PET image

Wang et al 2006 Systematic and Distributed Time-of-Flight List Mode PET Reconstruction

Data Corrections

- Power of PET is in quantification, which requires accurate **data corrections (non-TOF or TOF specific)** to be implemented
- With analytical algorithms such as filtered backprojection (FBP) the data are pre-corrected before reconstruction
- Corrections are incorporated in the reconstruction loop in iterative algorithms, such as ordered subset expectation maximization (OSEM):
  - Detector geometry, normalisation of detector efficiencies, detector dead-time
  - Attenuation, scatter, random events
  - Resolution recovery (PSF), TOF-specific corrections e.g. for scatter
- Calibration from counts to activity units (kBq/ml) and correcting for radioactive decay are also performed
- Post-smoothing (e.g. 3D Gaussian with FHWM in mm) is applied to control the noise in the images, although some expections apply (e.g. Q.Clear, blob-RAMLA)

Data Corrections in Image Reconstruction

Pre-2004

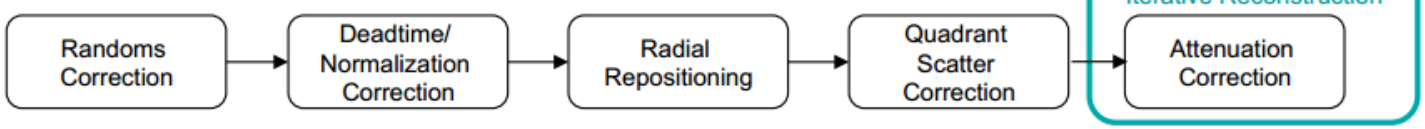

$$f_i^{n+1} = f_i^n \frac{1}{\sum_{j'=1}^{N_{LOR}} a_{j',i} / \alpha_{j'}} \sum_{j=1}^{N_{LOR}} a_{j,i} \frac{p_j}{\sum_{i'=1}^{P} a_{j,i'} f_{i'}^n}$$

$$i = 1, \ldots, P$$

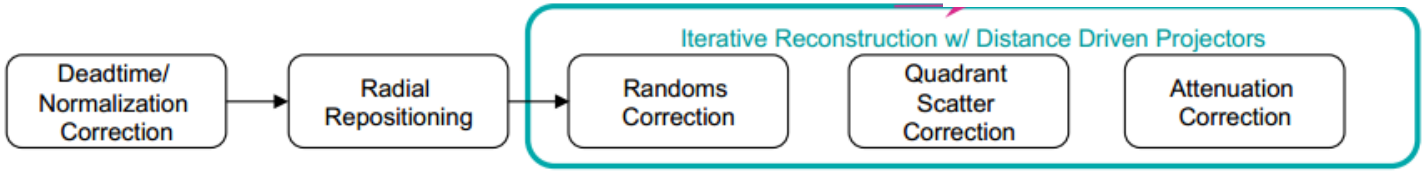

$$f_i^{n+1} = f_i^n \frac{1}{\sum_{j'=1}^{N_{LOR}} a_{j',i} / \alpha_{j'}} \sum_{j=1}^{N_{LOR}} a_{j,i} \frac{p_j + 2\bar{r}_j + \bar{s}_j}{\sum_{i'=1}^{P} a_{j,i'} f_{i'}^n + \alpha_j (2\bar{r}_j + \bar{s}_j)}$$

$$i = 1, \ldots, P$$

Mid-2007

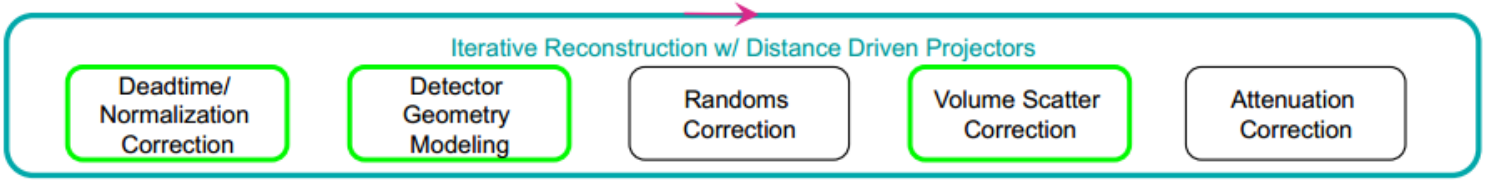

Practical Example
LM-OSEM

A relaxed List Mode Ordered Subset Expectation Maximization (LMOSEM) algorithm

$$\hat{f}_i^{k,m} = \hat{f}_i^{k,m-1} \left\{ (1-\lambda) + \frac{\lambda}{s_i} \sum_{j \in subset\ m} \eta_j^{atten} H_{ji}^{TOF} \frac{1/\eta_j^{multi}}{\eta_j^{atten} \sum_{n=0}^{N-1} H_{jn}^{TOF} \hat{f}_n^k + b_j^{add}} \right\}$$

Algorithm-specific lambda

Attenuation correction

System matrix, TOF-specific

$$where \quad s_i = \sum_{\text{all possible } j \in subset\ m} \eta_j^{atten} H_{ji}^{TOF}$$

$$\eta_j^{multi} = \eta_j^{xtaleff} \eta_j^{\det geom} \eta_j^{decay} \eta_j^{deadtime} \eta_j^{xtaltime}$$

$$b_j^{add} = \left(sc_j(\hat{f}^k, \mu) + r_j \right) / \eta_j^{\det geom}$$

Sensitivity image, TOF-specific correction

Multiplicative correction factors

Additive corrections: scatter, randoms

Reconstruction Algorithms

- Analytical vs Iterative
- FBP
- MLEM
- OSEM

Analytical Reconstruction Algorithms

- One way to represent the imaging system is with the following linear relationship:
  - p = Hf +n, where p is the set of projections, H is the known system model, f is the unknown image, and n is the error in the observations.

- Analytical reconstruction techniques use the inverse of the discrete Radon transform to solve this problem, offering a direct mathematical solution for the image f from measured projection p.
  - Advantages: **scales linearly** with the acquired counts
  - Disadvantages: system model H is assumed ideal, poor noise handling/propagation, streak artifacts

- **Background reading** (e.g. Two-dimensional central slice theorem):
  - Image Reconstruction Algorithms in PET, Michel Defrise, Paul E Kinahan and Christian J Michel
  - PET Image Reconstruction, Adam Alessio and Paul Kinahan

Iterative Reconstruction Techniques

- Iterative reconstruction:
  - Can account for the noise structure in the observations, include a realistic system model
  - Potentially more accurate estimate, at the cost of greater computational demands
  - **Non-linear behavior** => FBP is preferred in some quantitative measurements
  - Reduced (or none) streak artifacts

- Basic components:
  - Model for the image (pixels, voxels, blobs)
  - Model for the system H (characterizing the imaging system) that relates image to data (probability that an emission from voxel is detected in projection)
  - Model for the data (statistical relationship between the measurements and expected value, e.g. a Poisson model) => objective function
  - Governing principle that defines the ”best” image (e.g. Maximum Likelihood = ML)
  - Final component: **algorithm** that finds the best image estimate (e.g. an image, which is a solution of a maximization of an objective function => maximizes the Poisson-log likelihood function)
  - **In general, the algorithms themselves are only discussed/referred**
    - **Two widely used approaches for finding the ML estimate: MLEM and OSEM**
    - **Apply to both 2D and 3D data**

Filtered Backprojection (FBP)

- Most frequently used analytic reconstruction algorithm is the filtered backprojection (FBP) algorithm
- The goal of FBP reconstruction is to compute the the image f(x,y) from projections p(s,ϕ):

$$f(x,y) \approx \tilde{f}(x,y) = \int_0^{\pi} \mathcal{F}_1^{-1}\left\{W(v_s)|v_s|\mathcal{F}_1\left\{p(s,\phi)\right\}\right\}d\phi$$

- In algorithmic form:
  - 1D Fourier transform of p(s,ϕ)
  - Multiplication with a ramp filter v_s
  - Apply a smoothing function/window $W(v_s)$
  - Inverse Fourier transform of the filtered projections
  - Backproject across all angles to image space
- We will consider a 2D case in the next slides, specific considerations apply to 3D case => **homework** ☺

FBP, MATLAB Example Noiseless data

1. for all angles φ:
   a) 1D Fourier transform into frequency space
      $p(x_r, \varphi) \rightarrow P(\upsilon_{xr}, \varphi)$
   b) multiplication with ramp filter υ_{xr}:
      $P^F(\upsilon_{xr}, \varphi) = P(\upsilon_{xr}, \varphi)\, \upsilon_{xr}$
   c) inverse 1D Fourier transform of filtered projections into projection space:
      $P^F(\upsilon_{xr}, \varphi) \rightarrow p^F(x_r, \varphi)$
2. backprojection $f(x, y) = \int_0^P p^F(x_r, \varphi) d\varphi$

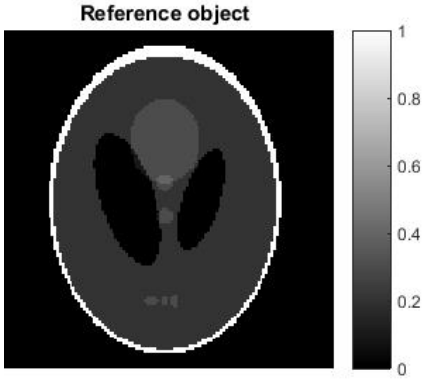

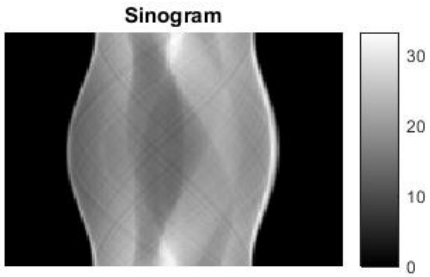

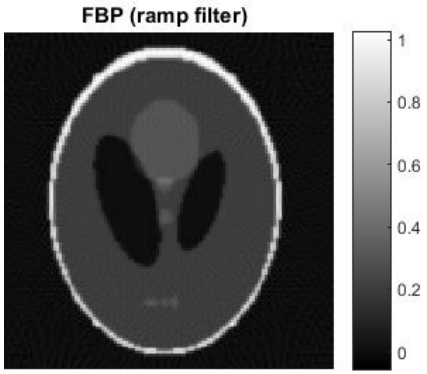

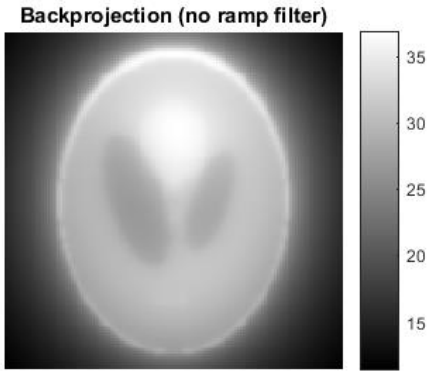

Performing mere backprojection versus applyinging backprojection after multiplication with a ramp filter in Fourier space.

FBP, MATLAB Example
Noisy Data

1. for all angles φ:
   a) 1D Fourier transform into frequency space
      $p(x_r, \varphi) \rightarrow P(\upsilon_{xr}, \varphi)$
   b) multiplication with ramp filter υ_{xr}:
      $P^F(\upsilon_{xr}, \varphi) = P(\upsilon_{xr}, \varphi)\, \upsilon_{xr}$
   c) inverse 1D Fourier transform of filtered projection into projection space:
      $P^F(\upsilon_{xr}, \varphi) \rightarrow p^F(x_r, \varphi)$
2. backprojection $f(x, y) = \int_0^P p^F(x_r, \varphi) d\varphi$

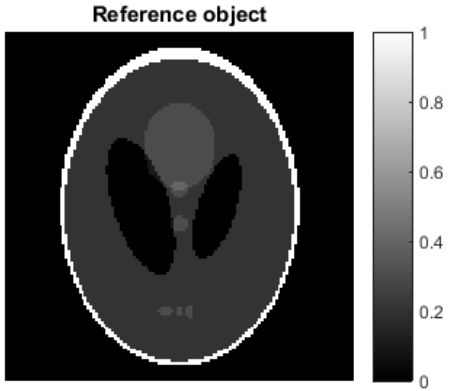

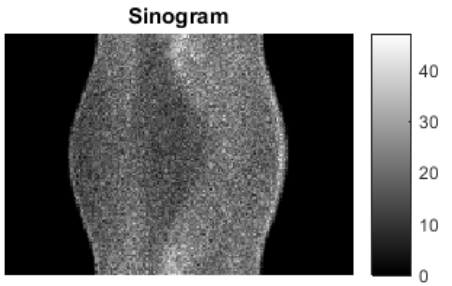

Applying additional filtering windows: Hann, Hamming, Shepp-Logan, etc.

Noise regularization is frequency selective (cutoff & window) => trade-off between resolution and noise.

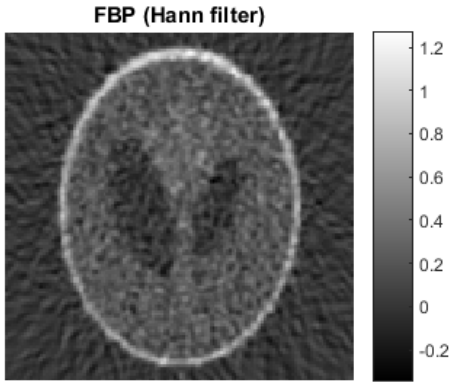

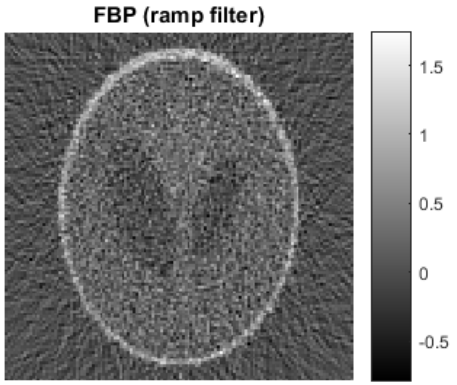

MLEM

Image and system model

$$\bar{p}_i = \sum_{j=1}^{N} H_{ij} f_j$$

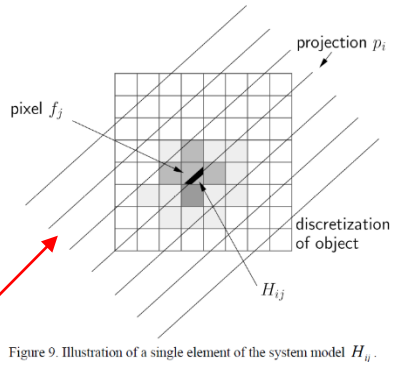

Figure 9. Illustration of a single element of the system model H_{ij}.

Detection process is modeled in the system matrix

Poisson Likelihood function, model for the data

$$\mathbf{L}(P = p \mid f) = \prod_{i=1}^{M} \frac{\bar{p}_i^{\,p_i} \exp(-\bar{p}_i)}{p_i!}.$$

Search for an image ***f*** that makes the measured data most likely to occur at argmax() of Poisson log-likelihood

Algorithm

$$f_j^{(n+1)} = \frac{\hat{f}_j^{(n)}}{\sum_{i'} H_{i'j}} \sum_i H_{ij} \frac{p_i}{\sum_k H_{ik} \hat{f}_k^{(n)}}$$

Image at nth iteration

Measured data (emission sinogram)

Updated image

System matrix

Forward projected image at nth iteration

MLEM
Example of One Iteration

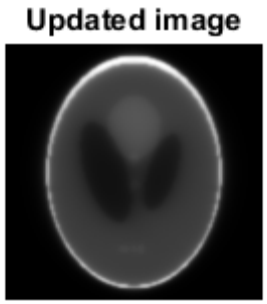

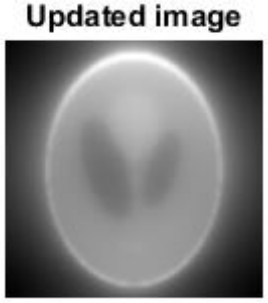

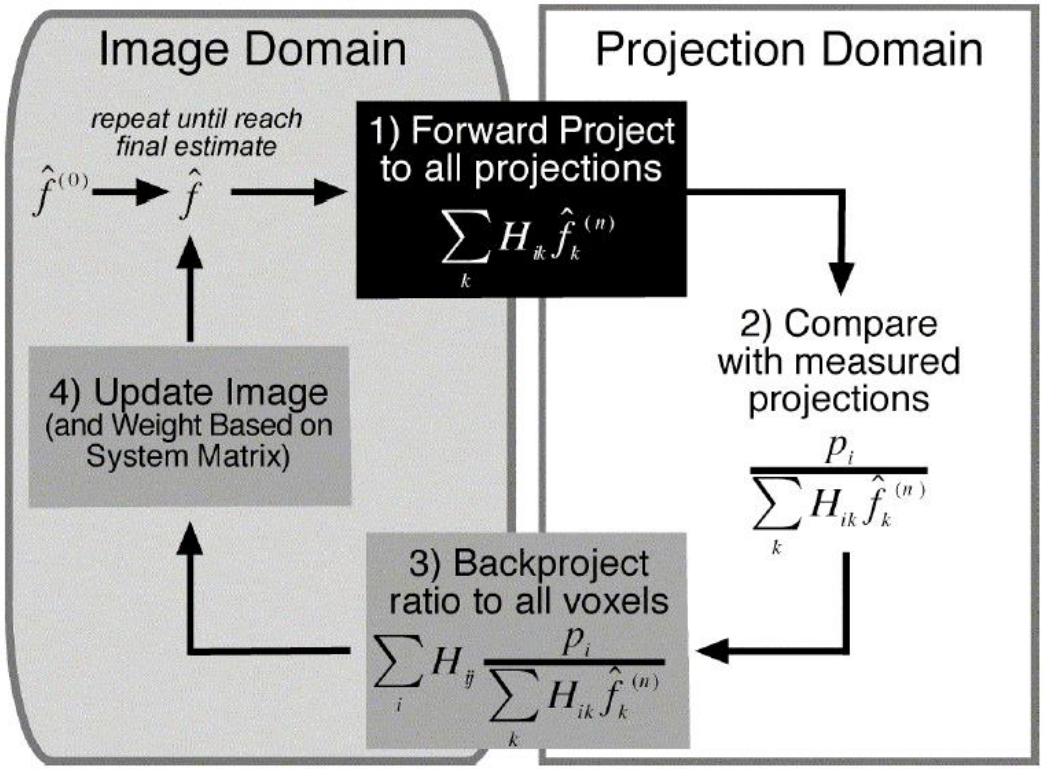

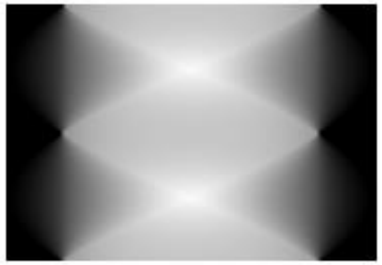

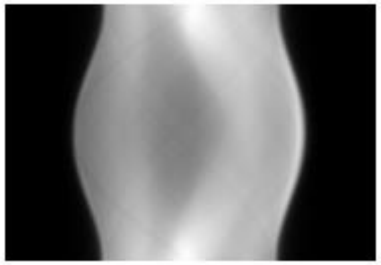

Figure 10. Flow diagram of the maximum likelihood-expectation maximization algorithm. Starting with an initial image guess ($\hat{f}^{(0)}$) in the upper left, the algorithm iteratively chooses new image estimates based on the measured projections, p.

OSEM

- Ordered Subsets Expectation Maximization (OSEM) was introduced to reduce reconstruction time of conventional MLEM.
- OSEM uses subsets of the entire dataset for each image update in the form:

$$f_j^{(n+1)} = \frac{\hat{f}_j^{(n)}}{\sum_{i' \in S_b} H_{i'j}} \sum_{i \in S_b} H_{ij} \frac{p_i}{\sum_k H_{ik} \hat{f}_k^{(n)}}$$

- The backprojection steps sum over only the projections in subset ***Sb*** of a total of ***b*** subsets, which are non-overlapping.
- Therefore, the image is updated during each subiteration and one complete iteration will have ***b*** image updates, allowing faster convergence over MLEM.
- When there is only one subset (***b* = 1**), OSEM is the same as MLEM. However, although OSEM resembles MLEM:
  - It is not guaranteed to converge to ML solution (in practice, convergence is similar to MLEM)
  - It has more image variance at the same bias level compared to MLEM

OSEM vs MLEM – FIGHT! MATLAB Example

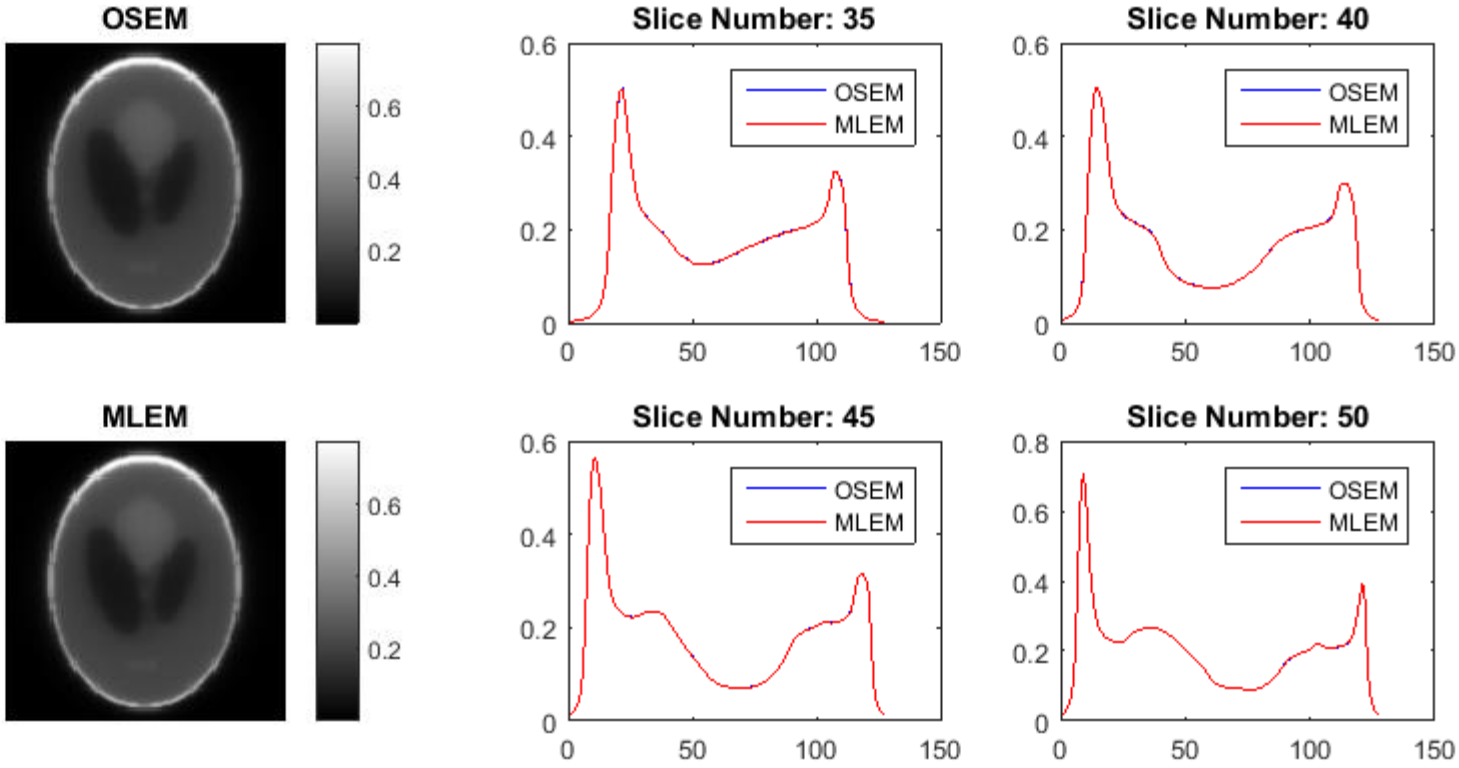

OSEM: 2 subsets, 4 iterations
MLEM: 8 iterations

OSEM vs MLEM – FIGHT! MATLAB Example

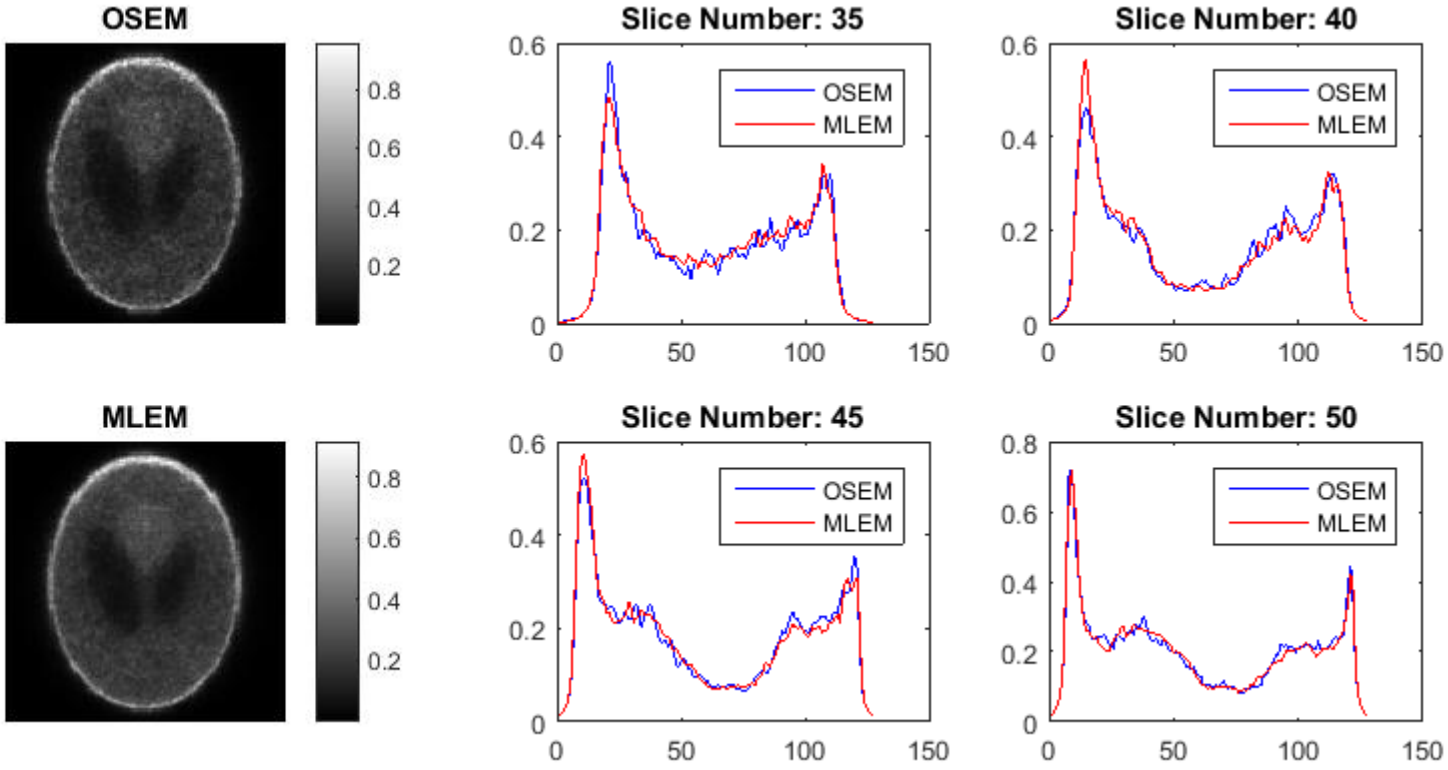

OSEM: 2 subsets, 4 iterations
MLEM: 8 iterations

OSEM vs MLEM – FIGHT! MATLAB Example

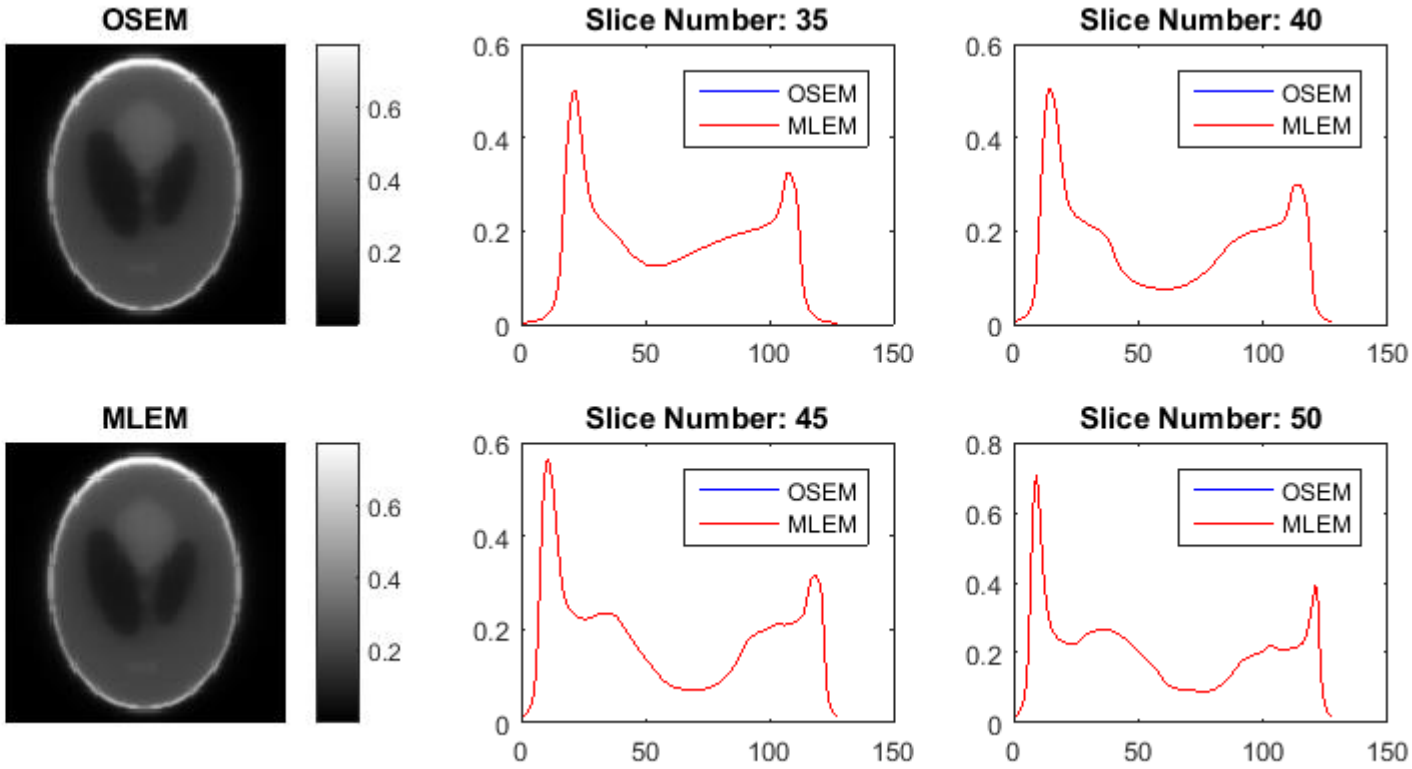

OSEM: 1 subset, 8 iterations
MLEM: 8 iterations

Thank You!

Turku PET Centre

Turun yliopisto
University of Turku

TYKS
TURUN YLIOPISTOLLINEN KESKUSSAIRAALA
TURKU UNIVERSITY HOSPITAL